Supplemental material

Post-sepsis immunosuppression depends on NKT cell regulation of mTOR/IFNγ in NK cells

Edy Y. Kim[1,2], Hadas Ner-Gaon[3], Jack Varon[1,2], Aidan M. Cullen[4], Jingyu Guo[4], Jiyoung Choi[1], Diana Barragan-Bradford[1], Angelica Higuera, Mayra Pinilla-Vera[1], Samuel A.P. Short[5], Antonio Arciniegas-Rubio[1], Tomoyoshi Tamura[1], David E. Leaf[5,2], Rebecca M. Baron[1,2], Tal Shay[3], Michael B. Brenner[2,4]#

[1]Pulmonary and Critical Care Medicine, Brigham and Women's Hospital
[2]Harvard Medical School
[3]Dept. of Life Sciences, Ben-Gurion University of the Negev
[4]Rheumatology, Immunology and Allergy, Brigham and Women's Hospital
[5]Division of Renal Medicine, Brigham and Women's Hospital

Table of contents

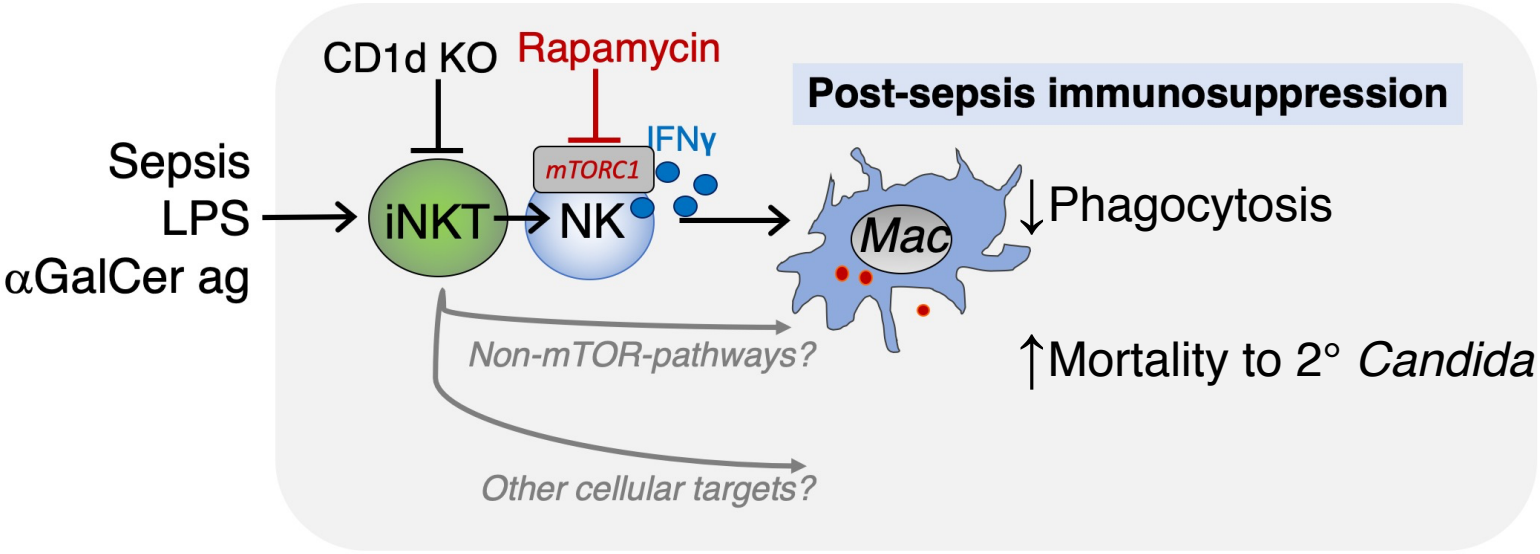

Supplemental Figure 1. Scheme: iNKT cells activate mTORC1 in NK cells to produce IFNγ and drive post-sepsis immunosuppression. IFNγ suppresses macrophage phagocytic function and increased susceptibility to secondary *Candida* infection. This NKT cell-mTOR-IFNγ pathway mediates NKT cell-dependent post-sepsis immunosuppression, but other pathways also likely contribute.

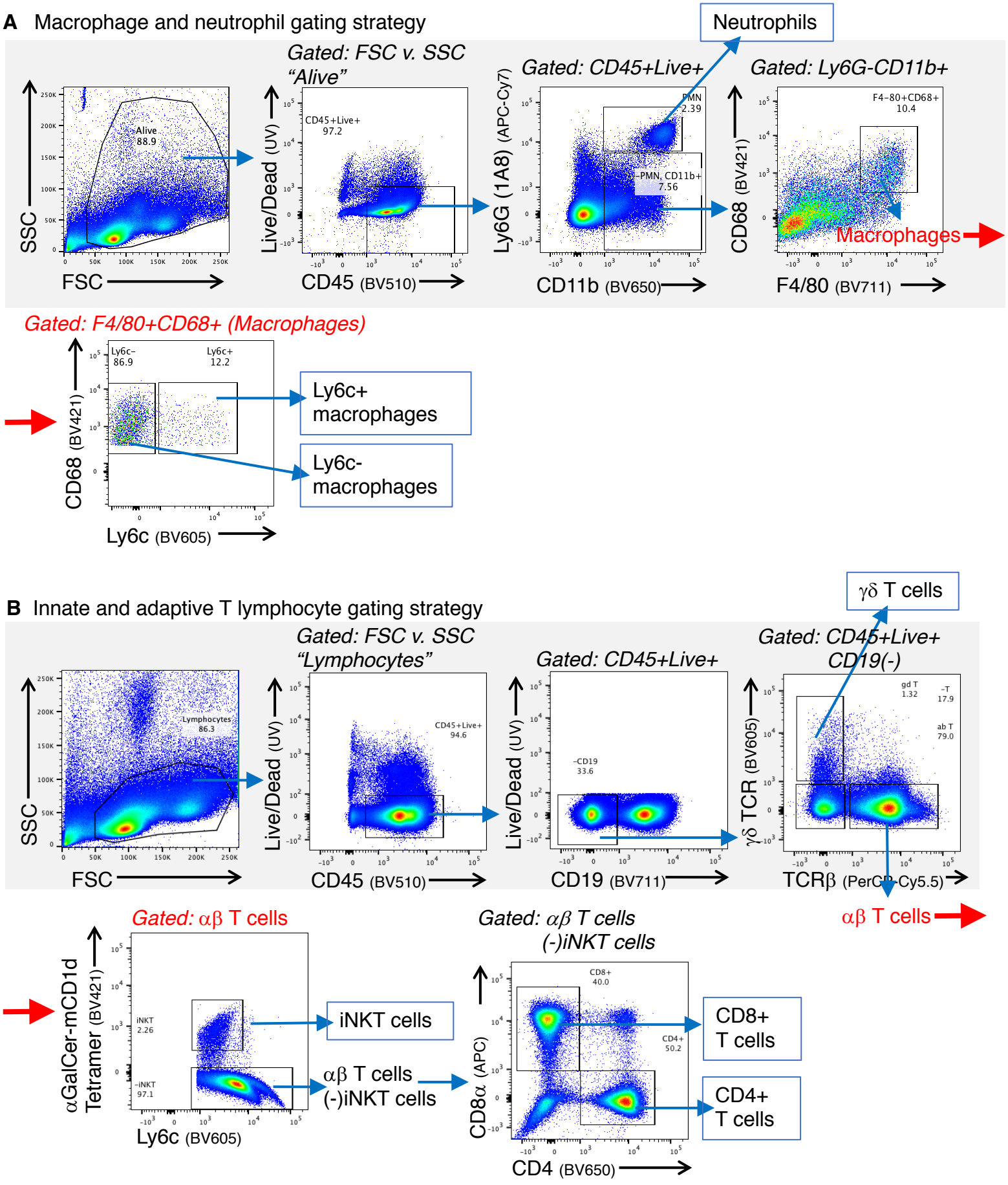

Supplemental Figure 2. Gating strategy for flow cytometry analysis. Representative WT naïve splenic cells are shown. **(A)** Ly6c+/- macrophage and neutrophil gating. **(B)** γδ T, iNKT, CD8+T and CD4+ T cell gating. **(C)** NK cell and NK1.1+ ILC gating.

C NK cell and NK1.1+ ILC gating strategy

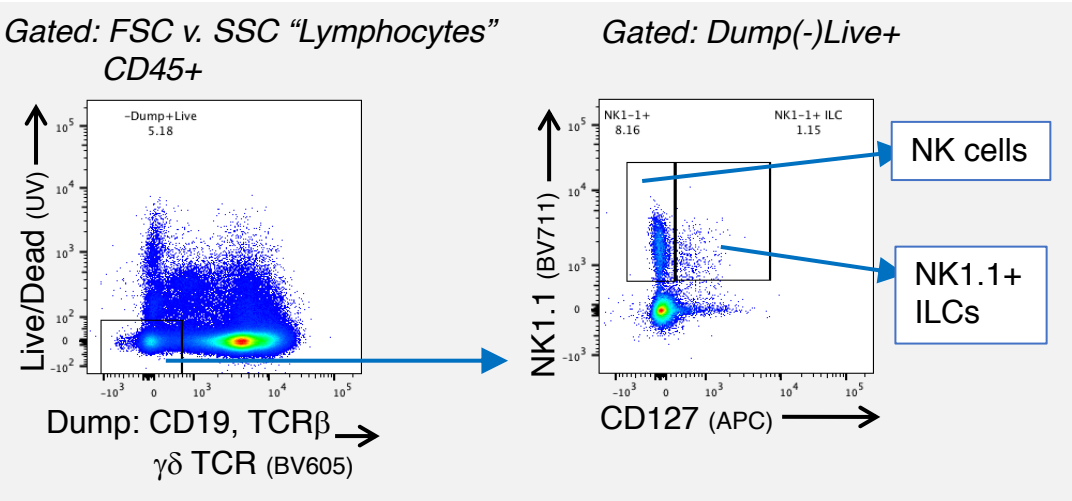

Supplemental Figure 2. Gating strategy for flow cytometry analysis. Representative WT naïve splenic cells are shown. **(A)** Ly6c+/- macrophage and neutrophil gating. **(B)** γδ T, iNKT, CD8+T and CD4+ T cell gating. **(C)** NK cell and NK1.1+ ILC gating.

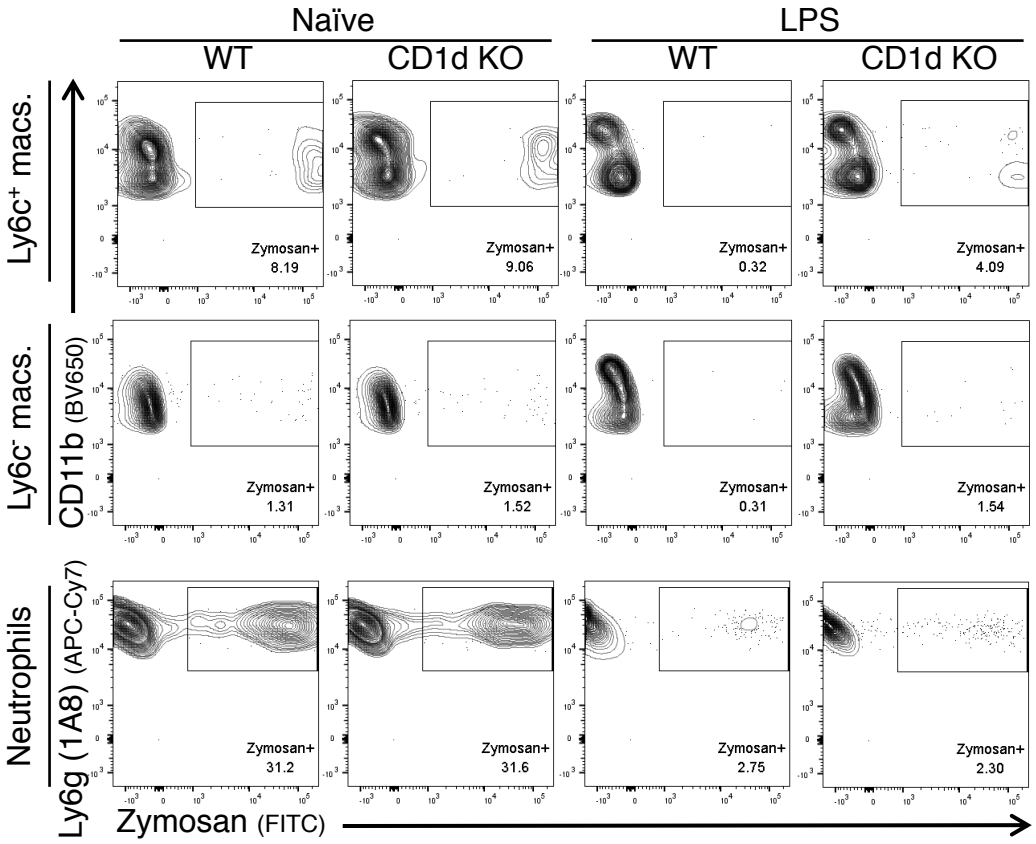

Supplemental Figure 3. NKT cell-deficient mice have improved splenic Ly6c+ macrophage function by in vivo phagocytosis assay during primary endotoxemia (representative flow cytometry plots for Fig. 3D). WT and CD1d KO mice were treated with saline or endotoxemia followed 18 hr later by opsonized zymosan-FITC i.v. Then, after 30 mins., splenic subsets were analyzed by flow cytometry. Ly6c+ macrophage plots are repeated from Fig. 3D.

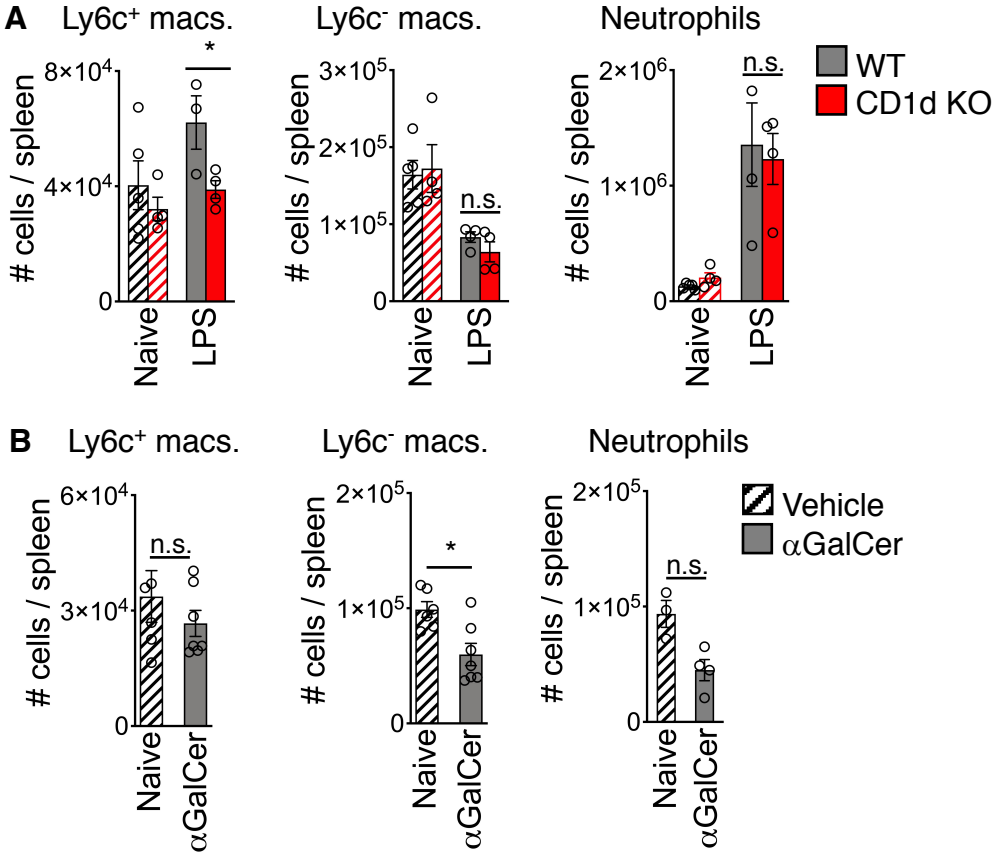

Supplemental Figure 4. Splenic cell numbers in endotoxemia or after selective activation of iNKT cells by αGalCer glycolipid antigen. Cell counts for splenic cell subsets. WT and CD1d KO mice were treated with saline ("Naïve") and either **(A)** LPS i.v. (n=3-5) or **(B)** αGalCer (macrophages n=5-7, neutrophils n=3). After 18 hr, splenic cell subsets were analyzed by flow cytometry. Mean±SEM shown. A:unpaired t-test; B:Ly6c+ macs.:unpaired t-test, Ly6c- macs. and neutrophils:Mann-Whitney. *p<0.05.

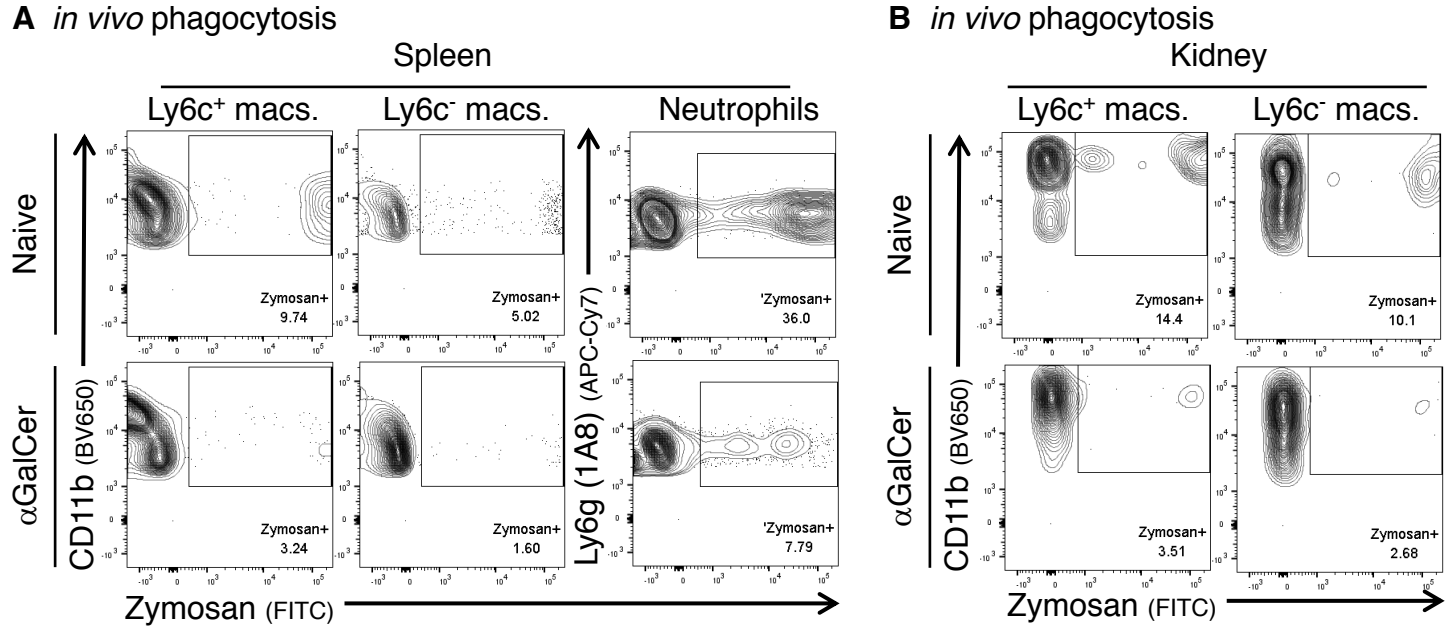

Supplemental Figure 5. Selective activation of iNKT cells with glycolipid antigen (αGalCer) impairs the phagocytic function of macrophages and neutrophils (flow cytometry plots for Figure 4C). In vivo phagocytosis assay. WT mice were treated with vehicle (naïve) or αGalCer 1ug i.p., then 18 hr later with opsonized zymosan-FITC i.v. After 30 mins., phagocytosis of immune cell subsets was assessed by flow cytometry in **(A)** spleen and **(B)** kidney. Plots for Ly6c+ macrophages are repeated from Figure 4C.

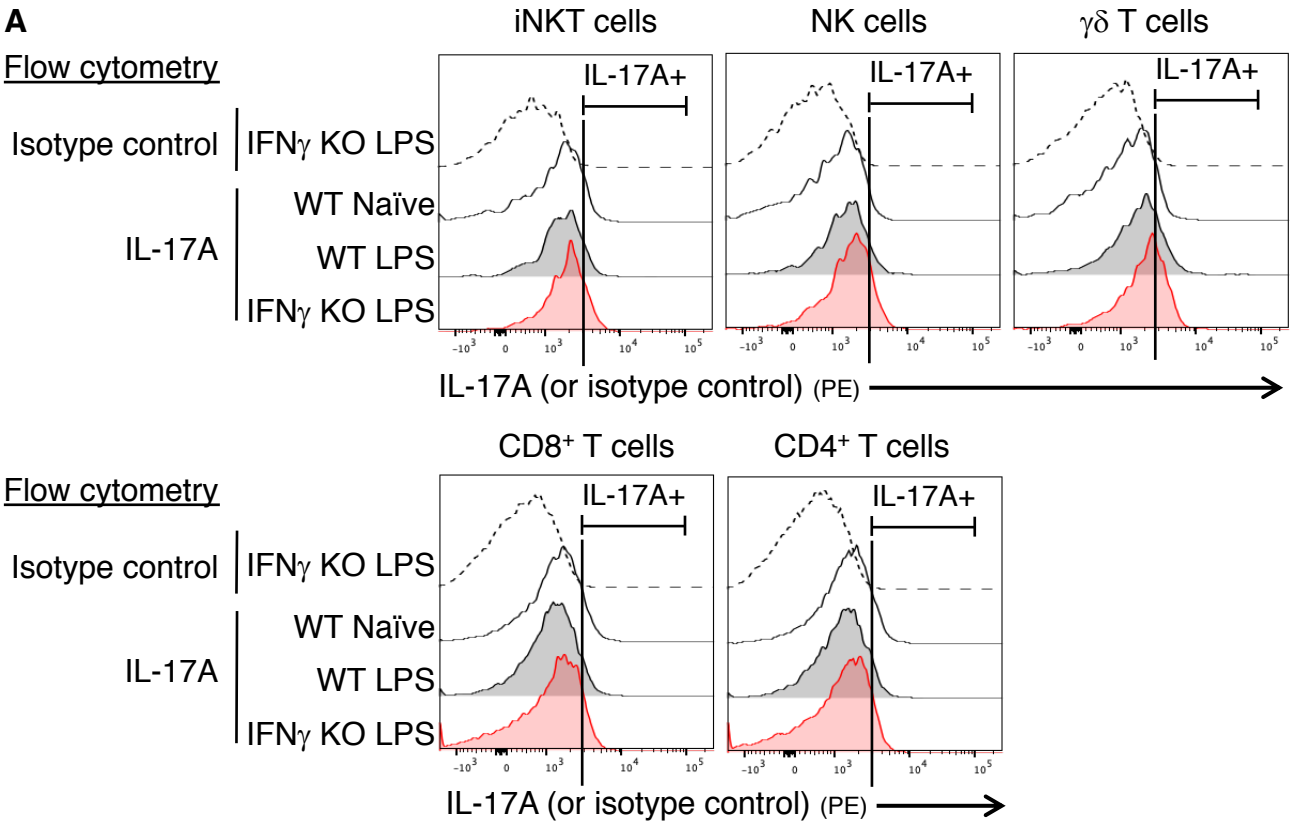

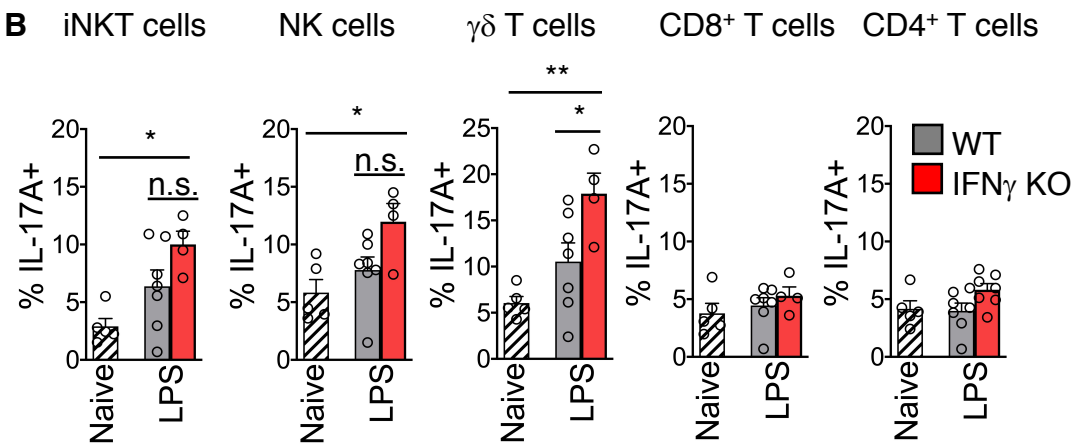

Supplemental Figure 6. IFNγ suppresses IL-17A production by innate T cells during endotoxemia. Percentage of IL-17A$^+$ cells during endotoxemia. WT or IFNγ KO mice were given LPS i.v. (or vehicle, "Naïve") (n=5-7 per group). 3 hr post-LPS, mice were given brefeldin A i.p.; 6 hr post-brefeldin, IL-17A was assessed by flow cytometry in splenic cell types (with isotype control antibody for IL-17A). **(A)** Representative flow cytometry histograms. **(B)** Quantification of % IL-17A+ cells. For bar graphs, mean±SEM shown. CD8+ T cells:Kruskal-Wallis; Other cell types:unpaired t-test. *p<0.05, **p<0.01.

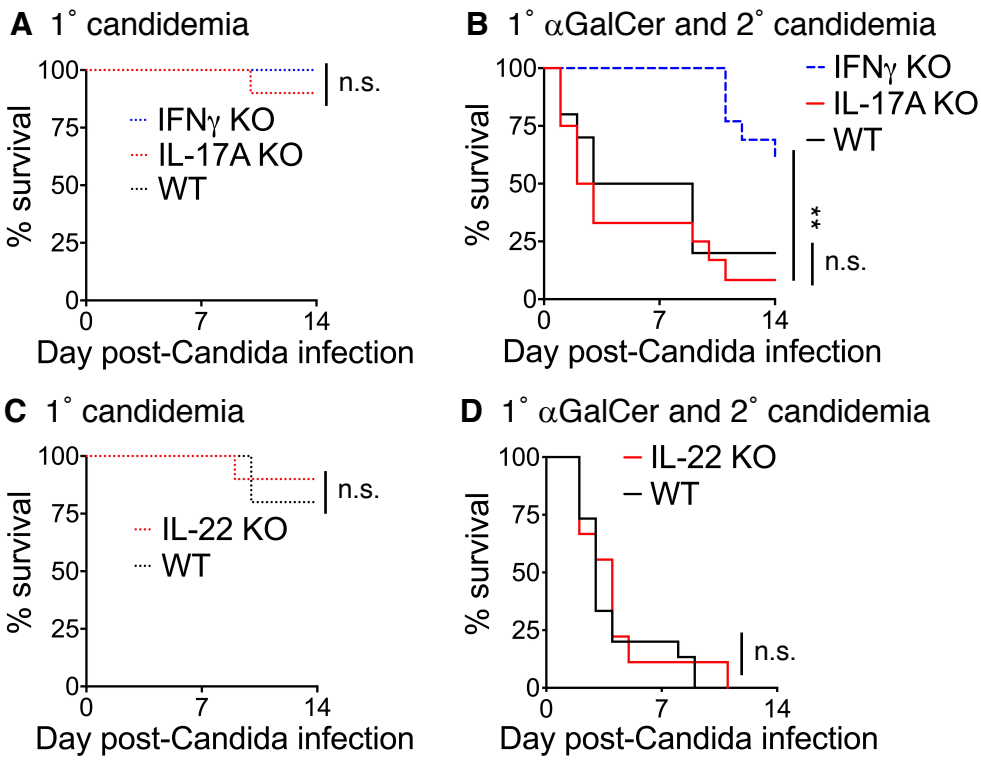

Supplemental Figure 7. IL-17A or IL-22 are not necessary for iNKT cell-driven susceptibility to secondary candidemia. (A, C) Survival curves for primary candidemia: WT, IL-17A KO and IFNγ KO mice; or WT and IL-22 KO mice were infected with low-dose *Candida* i.v. only. (A:WT/IL-17A KO:n=10, IFNγ KO n=5 per group; C: WT:n=5, IL-22 KO n=10 per group). **(B, D)** Survival curves for iNKT cell activation and secondary candidemia. WT, IL-17A KO and IFNγ KO mice; or WT and IL-22 KO mice received αGalCer i.p. then 18 hr mice later received a secondary infection of *Candida* i.v. (B:n=14; D: WT:n=15, IL-22 KO:n=9 per group). A-D:Log-rank. **p<0.001.

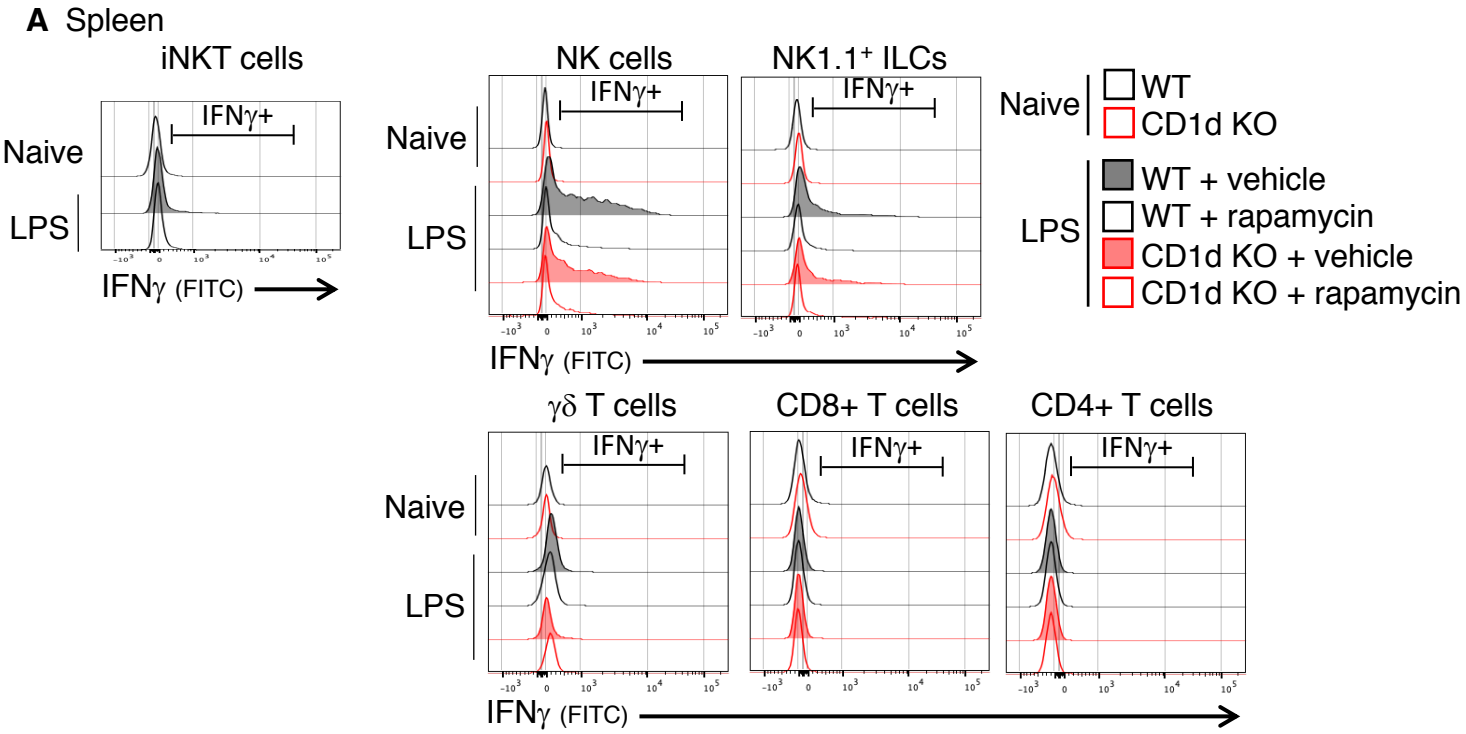

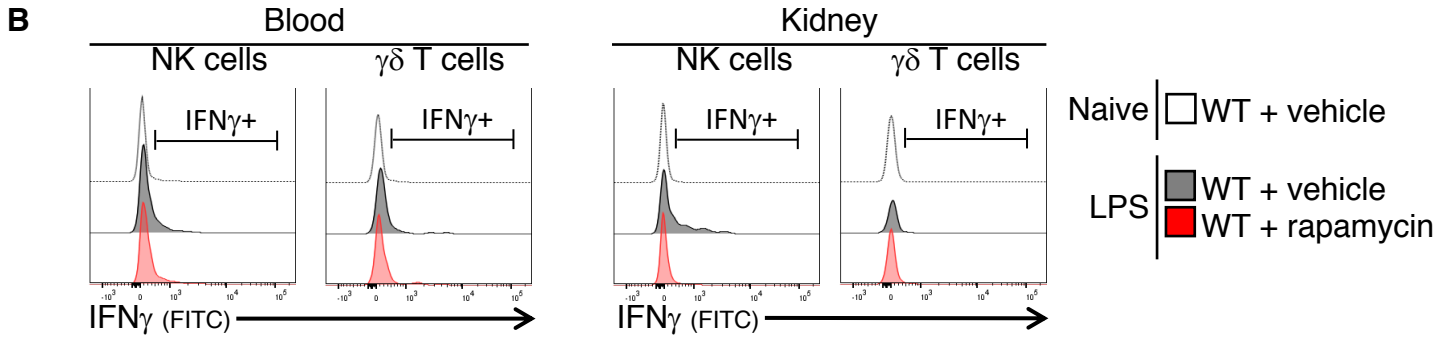

Supplemental Figure 8. iNKT cells regulate mTOR / IFNγ in NK cells during endotoxemia (flow cytometry plots for Figure 5E). WT or CD1d KO mice were treated with rapamycin i.p. (or vehicle) and then 3 hr later received LPS i.v. (or vehicle). 3 hr later, mice were given brefeldin A i.p. At 6 hr post-brefeldin, % IFNγ+ was assessed in by flow cytometry in immune cell subsets from **(A)** spleen and **(B)** blood and kidney.

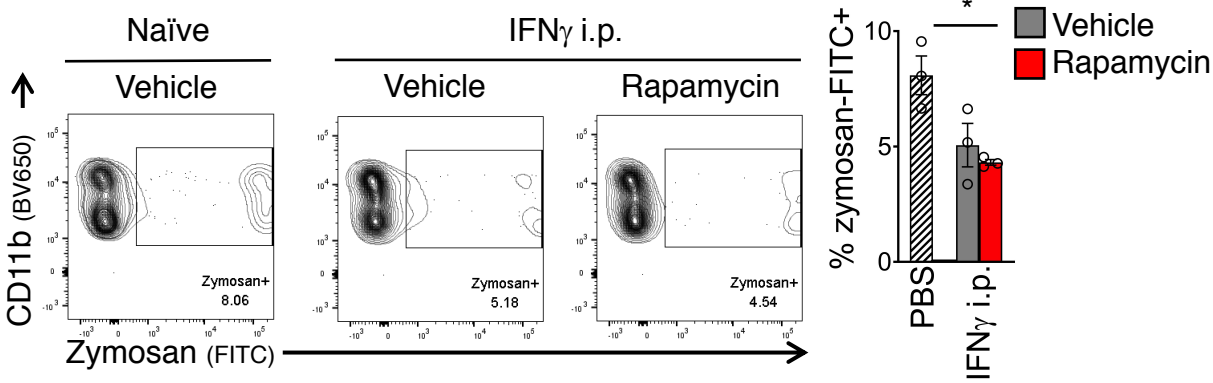

Supplemental Figure 9. Suppression of phagocytic function by exogenous IFNγ treatment is independent of mTOR. In vivo phagocytosis assay. IFNγ KO mice were treated with rapamycin i.p. (or vehicle). 3 hr later, IFNγ 1ug i.p. or vehicle were administered to mice. 18 hr later, mice were challenged with opsonized zymosan-FITC i.v. and then phagocytosis assessed after 30 mins in splenic Ly6c+ macrophages by flow cytometry. (n=3 per group). For bar graph, mean±SEM shown. 1-way ANOVA. *p<0.05.

A Kidney *in vivo* phagocytosis: post-1º αGalCer (Figure 6E)

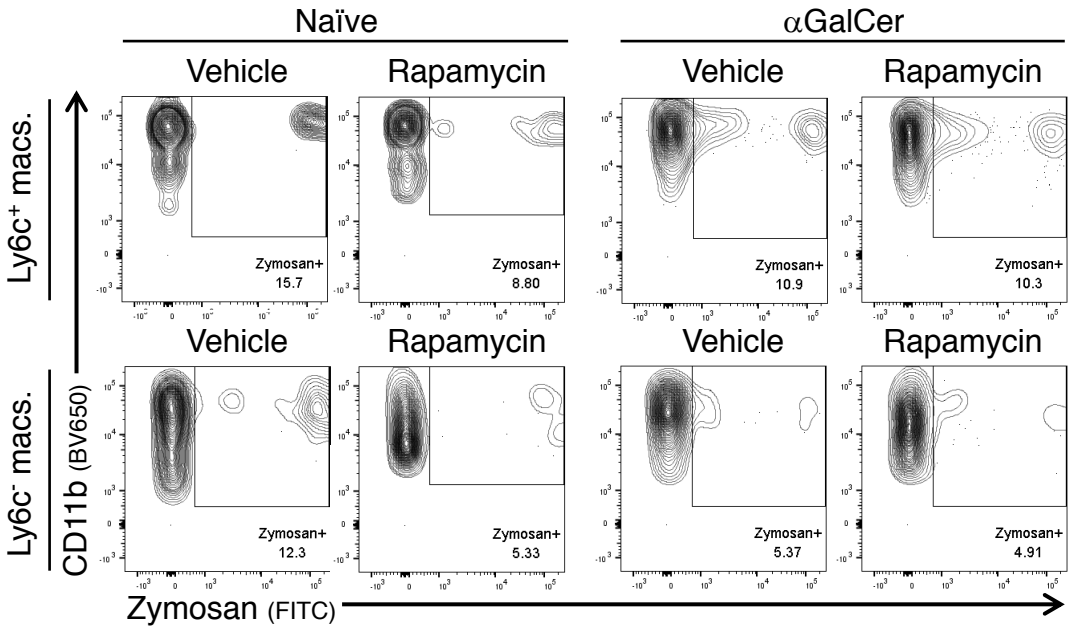

B Kidney *in vivo* phagocytosis: post-2º candidemia (Figure 6F)

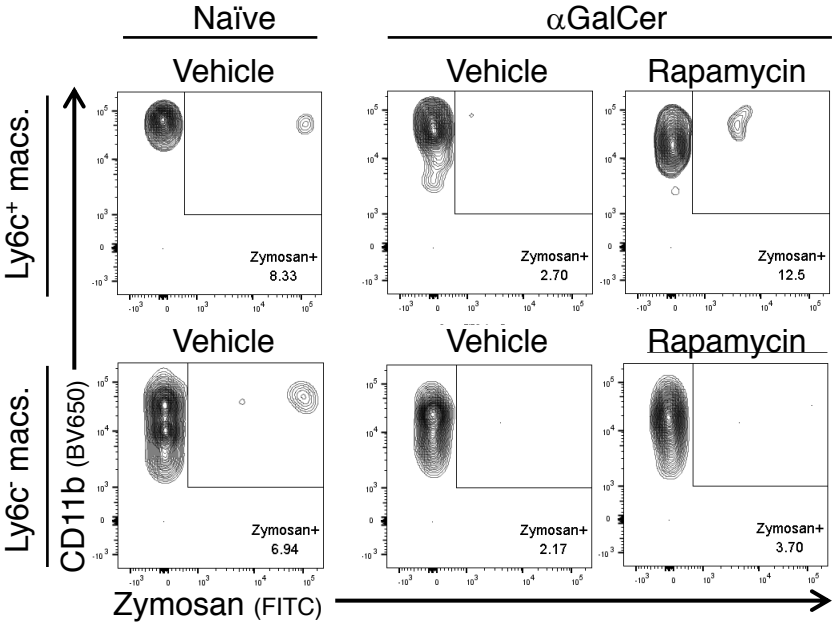

Supplemental Figure 10. Selective activation of iNKT cells by the glycolipid antigen αGalCer impairs macrophage phagocytosis via mTOR (flow cytometry plots for Figures 6E-F). *In vivo* phagocytosis assay. Glycolipid αGalCer i.p. (or vehicle) was administered to WT mice. At 3 hr and 15 hr post-aGalCer i.p. (or vehicle), mice were treated with rapamycin i.p. (or vehicle). **(A)** Post-1º αGalCer: At 18 hr post-αGalCer, mice were challenged with opsonized zymosan-FITC, and 30 mins. later phagocytosis assessed by flow cytometry in kidney macrophages (quantified as Figure 6E). **(B)** WT mice were treated with αGalCer then rapamycin as in (A). At 18 hr post-αGalCer, mice were infected with low-dose *Candida* i.v. At 1 day post-*Candida* infection, mice were challenged with opsonized zymosan-FITC and 30 mins. phagocytosis assessed by flow cytometry in kidney macrophages (quantified as Figure 6F).

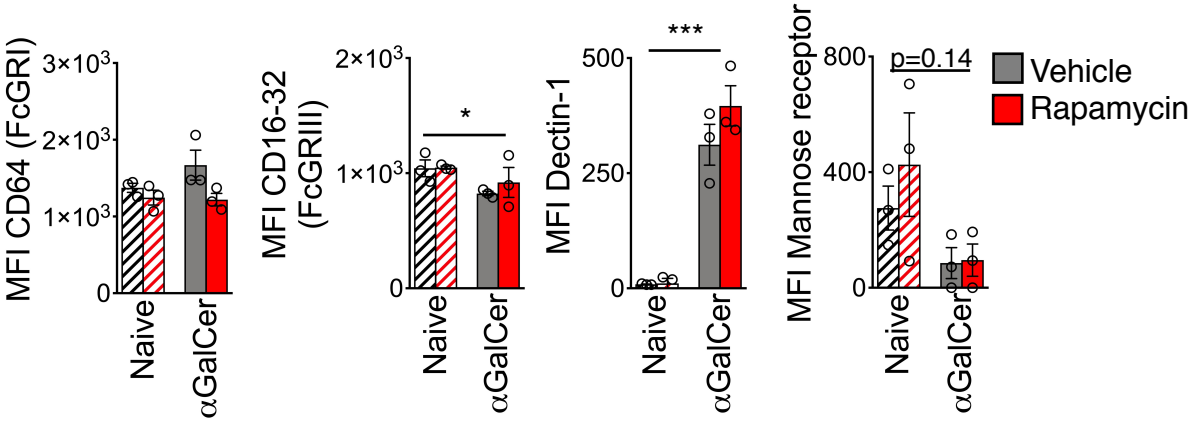

Supplemental Figure 11. Expression of cell surface receptors on splenic Ly6c$^+$ macrophages after selective activation of iNKT cells by glyclolipid antigen αGalCer ± rapamycin. In vivo phagocytosis assay. αGalCer i.p. (or vehicle, "Naïve") was administered to WT mice. At 3 hr and 15 hr post-αGalCer i.p. (or vehicle), mice were treated with rapamycin i.p. (or "Vehicle"). At 18 hr post-αGalCer (or vehicle), receptor expression was assessed by flow cytometry on splenic Ly6c$^+$ macrophages. (n=3 per group). Mean±SEM shown. 1-way ANOVA. *p<0.05; ***p<0.0001.

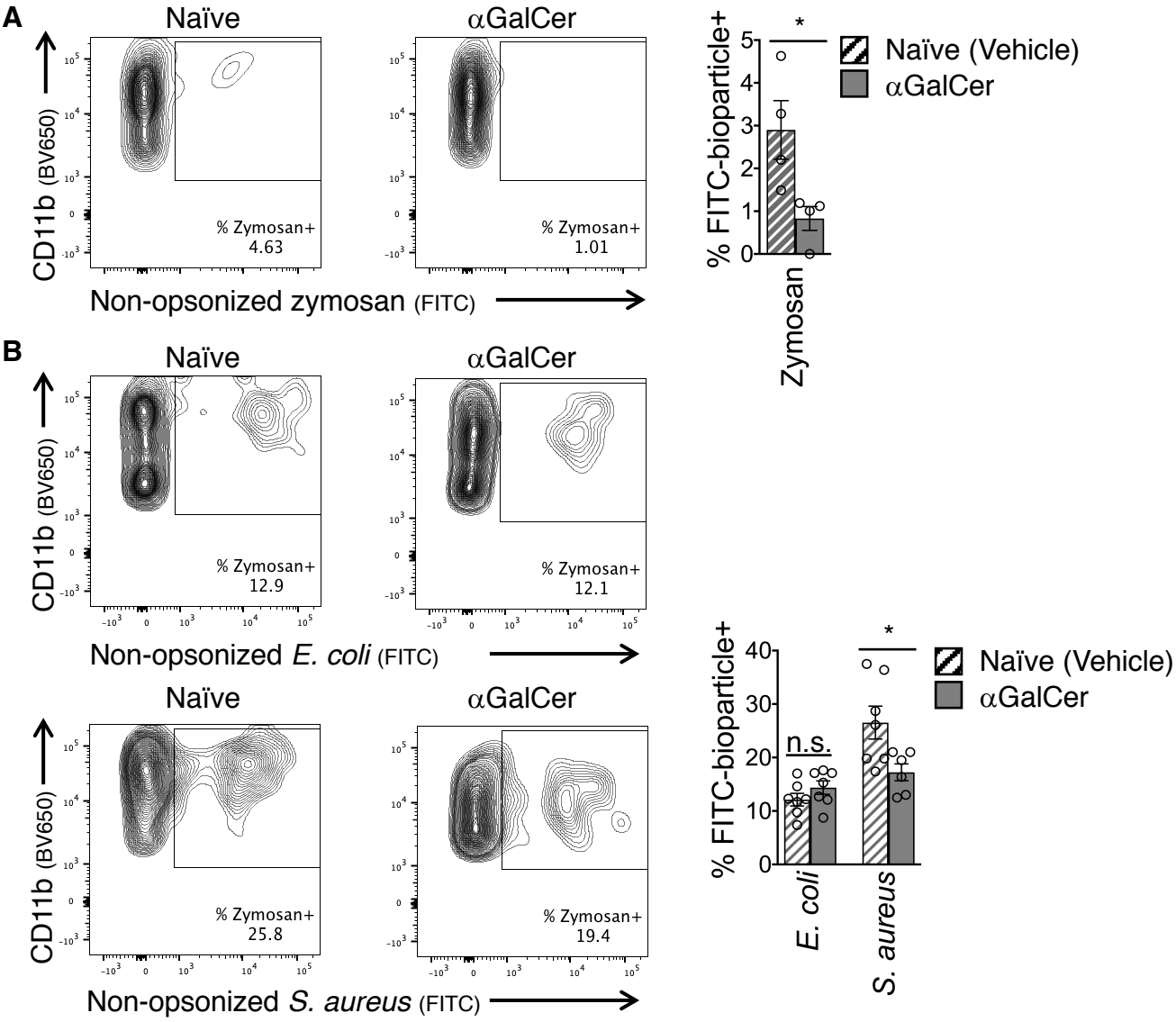

Supplemental Figure 12. Selective NKT cell activation by glycolipid antigen αGalCer suppresses in vivo phagocytosis of non-opsonized zymosan and *S. aureus* bioparticles. In vivo phagocytosis assay. αGalCer i.p. (or vehicle, "Naïve") was administered to WT mice. At 18 hr post-αGalCer (or vehicle), mice were challenged with non-opsonized, FITC-labelled bioparticles: **(A)** zymosan-FITC i.v. (n=4 per group); **(B)** killed *E. coli* or killed *S. aureus* i.v. (n=6-7). After 30 min., phagocytosis by splenic Ly6c$^+$ macrophages were assessed by flow cytometry. For bar graphs, mean±SEM shown. A:Mann-Whitney; B:unpaired t-test. *p<0.05.

Supplemental Table 1. Clinical characteristics of septic patients in Figure 1A. Septic patients were prospectively enrolled in registries of critical illness. Inclusion criteria were sepsis and enrollment within 48 hr of sepsis diagnosis and admission to the ICU. Patients that already had *Candida* infection at the time of enrollment were excluded. Patients were grouped by continued absence of secondary *Candida* infection or later development of secondary *Candida* infection. IFNg levels were measured by ELISA in plasma taken on day of enrollment (Fig. 1A). Statistical analysis of categorical variables (sex, hypotension, ICU type, source of infection) by Chi-square test. All other variables by unpaired t-test, except lactate by Mann-Whitney.

	Sepsis only	**1° Sepsis and 2° *Candida***	P-value
Number of patients	19	12	
Age	63.9 ± 15.1	58.3 ± 14.3	0.36
Sex	11 (56%)	6 (50%)	0.67
Hypotension	15 (79%)	9 (75%)	0.80
SOFA	10.9 ± 4.7	10.5 ± 4.5	0.99
APACHE	30.0 ± 7.4	29.6 ± 7.9	0.69
Max HR	103 ± 28	128 ± 23	0.01
Temp	99.8 ± 1.4	99.5 ± 2.0	0.46
WBC	18.30 ± 12.18	18.77 ± 9.68	0.88
Lactate	3.7 ± 2.7	4.2 ± 2.7	0.28
ICU type			
MICU	13 (68%)	5 (42%)	0.14
SICU	6 (32%)	7 (58%)	
Source of infection			
Pneumonia	12 (63%)	5 (42%)	0.047
Genitourinary	2 (11%)	0 (0%)	
Abdominal	4 (21%)	4 (33%)	
Skin and Soft Tissue	1 (5%)	0 (0%)	
Mediastinal/ Pleural	0 (0%)	3 (25%)	
Source of candida culture			
Bloodstream	n/a	5 (42%)	n/a
Abdominal Fluid/Abscess	n/a	4 (33%)	
Pleural fluid	n/a	3 (25%)	

Supplemental Table 2. Cultured organisms causing primary sepsis for patients in Figure 1A. For the patients in Figure 1A and Supplemental Table 1, the cultured organisms (if any) that caused their sepsis are shown. P-value for % (+) culture assessed by Chi-squared.

	Sepsis only		**1° Sepsis and 2° *Candida***		
	# of patients (%)	Organism (# patients)	# of patients (%)	Organism (# patients)	P-value
Organism not cultured	8 (42%)		7 (58%)		0.38
(+) Sputum cultures	5 (26%)	*S. Aureus* (4)	2 (17%)	*S. Aureus* (2)	0.53
		E. Coli (1)			
(+) Blood cultures	5 (26%)	*Streptococcus* (1)	2 (17%)	*E Faecalis* (1)	0.53
		S. Aureus (1)		*Acinetobacter* (1)	
		E. Coli (1)			
		E. Faecalis (1)			
		Klebsiella (1)			
(+) Urine cultures	3 (16%)	*E. Coli* (2)	0 (0%)		0.15
		S. Aureus (1)			
(+) Pleural fluid culture	0 (0%)		1 (8%)	*Streptococcus* (1)	0.20